STRUCTURAL AND OPTICAL PROPERTIES OF Tm$_2$O$_3$-DOPED ZINC BOROTELLURITE GLASS SYSTEM

L. HASNIMULYATI[a], M. K. HALIMAH[a,*], A. ZAKARIA[a], S. A. HALIM[a], M. ISHAK[b], C. EEVON[a]
[a]*Department of Physics, Faculty of Science, Universiti Putra Malaysia, 43400 UPM Serdang, Selangor*
[b]*Technical Support Division, Malaysian Institute for Nuclear Technology Research (MINT), Bangi, Kajang, Malaysia*

Thulium doped zinc borotellurite glasses with composition $\{[(TeO_2)_{0.7}(B_2O_3)_{0.3}]_{0.7}[ZnO]_{0.3}\}_{1-x}\{Tm_2O_3\}_x$ were synthesized using melt-quenching technique. The values of x varied from 0.01 to 0.05 mol. The density and molar volume of the glass samples were found to increase with increased concentration of thulium oxide. FTIR analysis showed the existence of TeO$_4$, BO$_3$ and BO$_4$ structural units in the glass network as well as the formation of bridging oxygens. XRD patterns confirmed the amorphous nature of the glass and were supported by the absence of sharp edges in the absorption spectra. All the optical data was found to vary with the concentration of Tm$_2$O$_3$. The direct and indirect optical band gap was in the range of 4.19 to 4.38 eV and 3.62 to 3.79 eV respectively. The trend for refractive index, molar refraction and molar polarizability was in opposite trend to the optical band gap and Urbach energy due to the variation of non-bridging oxygens (NBOs), increment of cross-link density, and also the existence of free electrons in the glass system.

1. Introduction

The researches done on rare-earth doped glasses have been growing intensively due to its wide applications not only for doors and windows but also for optical, photonic, and electronic devices. Tellurite glass has many advantages such as low melting point, high refractive index, high dielectric constant, and good infrared transmission which causes it to be one of the most interesting materials to be studied [1]. However, tellurite glass can only be formed with the addition of alkali, alkaline earth, and transitional metal oxides or other glass formers. Hence, this makes it compulsory for the addition of other chemical oxides to tellurium oxide in order to produce glass. As a result, the addition of chemical oxides will cause changes to the properties of the pure tellurite glass.

The addition of metal oxides to tellurite glass was found to produce high transparent glass without the addition of glass formers. Besides that, it can enhance the optical behavior of the glass and make it a promising material for non-linear optical devices, optical fiber amplifiers, electronic optical switches and etc. According to the research done by Azlan et al. (2013) [2], zinc oxide can be used to enhance the properties of tellurite glass by increasing the glass stability, glass forming ability, refractive index and at the same time decrease the melting point as well as optical band gap. Furthermore, ZnO can act both as network modifier and network former by the formation of ZnO$_4$.

Previous studies done by Gebavi (2009) [3] stated that thulium oxide acts as a network modifier and reduces Te coordination. The same reaction occurred when Zn, Ba and Er were added. In addition, the refractive index was found to significantly reduce by the inclusion of Tm

---

*Corresponding author: halimahmk@upm.edu.my

ions. Another research done by Tian et al. (2010) [4] reported that Tm^{3+} ions occupied the network sites as modifying oxides and stabilizing NBO bonds while Cho et al. (2000) [5] claimed that Tm^{3+}-doped tellurite glasses appear to be an excellent candidate for efficient optical fiber amplifiers at 1.47 µm region.

In this present article, the effect of thulium oxide to structural and optical properties of zinc borotellurite glass was investigated. This study is done in order to provide more data on Tm-doped glass and make it suitable to be used for laser and optical devices. It is expected that the addition of thulium oxide in the glass network will enhance the optical properties of the glass by lowering the optical band gap, increasing the refractive index and also its molar polarizability.

2. Experimental Details

2.1 Samples preparation

The quaternary glass system with composition $\{[(TeO_2)_{0.7}(B_2O_3)_{0.3}]_{0.7}[ZnO]_{0.3}\}_{1-x}\{Tm_2O_3\}_x$ where x = 0.01, 0.02, 0.03, 0.04 and 0.05 mol were prepared by using melt quenching technique. The chemical oxides of TeO_2, B_2O_3, ZnO and Tm_2O_3 with purity more than 97% were weighed to get the right proportion that are needed to synthesize the sample. After that, the chemical oxides were mixed, stirred, and ground to obtain a homogeneous mixture. The mixture was then pre-heated at 400°C and melted at 900°C using two different furnaces each for an hour. Next, the molten was poured into a stainless steel mould that had been pre-heated at 400°C and put in the furnace again for annealing process. This process was done to reduce any residual thermal stresses in the glass sample. After two hours, the furnace was turned off and the glass sample was left to cool down to room temperature. Lastly, the sample was cut to 2 mm thickness with low speed saw machine and then polished to get a parallel and clear surface. Excessive samples were grounded into powder form for Fourier Transform Infrared Spectroscopy (FTIR) and X-ray Diffraction (XRD) testing.

2.2 Sample characterization

The density of the glass samples was determined by using Electronic Densimeter MD-300S that operated based on Archimedes principle with distilled water as the immersion fluid. The value then can be calculated using the following relation:

$$\rho = \frac{m_a}{m_a - m_w} \rho_w \tag{1}$$

where ρ is the density of the sample, ρ_w is the density of water, m_a is the mass of sample in the air and m_w is the mass of sample in water. After that, molar volume can be calculated using equation:

$$V_m = \frac{M}{\rho} \tag{2}$$

where V_m is the molar volume and M is the total molecular weight.

The optical absorption of the glass samples were tested using UV–VIS spectrophotometer with wavelength in the range of 200 until 800 nm. Using these spectra, the absorption coefficient can be calculated using the equation as stated below [6]:

$$\alpha(\omega) = 2.303 \frac{A}{d} \tag{3}$$

where α is the absorption coefficient, A is the absorbance and d is the thickness of sample in cm. Next, optical band gap of the glass can be calculated using the known Mott–Davis equation:

$$\alpha(\omega) = \frac{B(\hbar\omega - E_{opt})^r}{\hbar\omega} \tag{4}$$

where B is the band tailing parameter, E_{opt} is the optical band gap, $\hbar\omega$ is the incident photon energy while r is the index number used to decide the nature of the interband electronic transition causing the absorption (r=1/2 for direct allowed transition and r=2 for indirect allowed transition) [7]. Based on this equation, the graphs of $(\alpha\hbar\omega)^2$ and $(\alpha\hbar\omega)^{1/2}$ vs $\hbar\omega$ can be plotted and the value of optical band gap is the extrapolation of the linear region in these two graphs.

In addition, Urbach energy is another optical parameter that can be attained from the absorption spectra. Referring to the equation from Urbach rule, it is obtained by calculating the reciprocal of slope in the graph of natural logarithm of $\alpha(\omega)$ as a function of photon energy, $\hbar\omega$:

$$\alpha(\omega) = \alpha_0 \, exp\left(\frac{\hbar\omega}{\Delta E}\right) \tag{5}$$

where α_0 is constant and ΔE is the Urbach energy. Besides, refractive index, molar refraction, and molar polarizability each can be calculated using the equations as follows:

$$1 - \frac{n^2-1}{n^2+2} = \left(\frac{E_{opt}}{20}\right)^{\frac{1}{2}} \tag{6}$$

$$R_m = V_m \left(\frac{n^2-1}{n^2+1}\right) \tag{7}$$

$$R_m = \frac{4}{3}\pi N_A \alpha_m \tag{8}$$

where n is the refractive index, R_m is the molar refraction, N_A is the Avogadro constant and α_m is the molar polarizability.

For structural properties, FTIR and XRD testing were done to investigate the structural units present and to confirm the amorphous nature of the glass.

3. Results and discussion

Fig. 1 shows the density and molar volume of thulium doped zinc borotellurite glass. Both of these parameters were found to increase with the addition of Tm_2O_3. The increase in density might be due to high molecular weight of thulium oxide compared to the other chemical oxides added [8]. As Tm was incorporated into the glass network, it caused the total molecular weight of the glass to increase. Since density is directly proportional to mass, the density of the glass was also elevated [9]. Besides that, the low ionic radii of Tm ion enable it to fill the interstitial spaces of the glass network and thus producing a compact glass. The conversion of structural units from TeO_3 to TeO_4 and BO_3 to BO_4 also contribute to the compaction as will be explained later. In terms of molar volume, the increment attributed to the large bond length and higher coordination number of Tm_2O_3 which thus leads to the growth of free volume inside the glass network. According to Rada et al. (2011) [10], the formation of non-bridging oxygens (NBOs) also caused the network to expand.
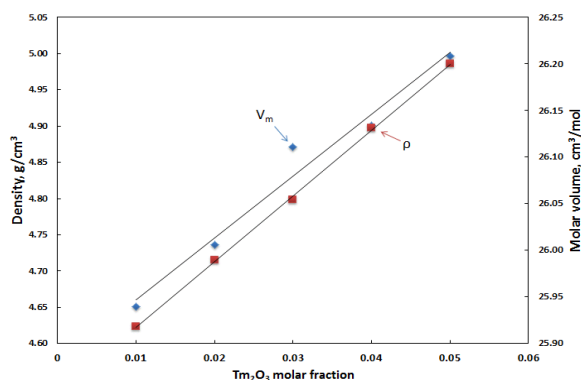
Fig. 1 Density and molar volume of {[(TeO$_2$)$_{0.7}$(B$_2$O$_3$)$_{0.3}$]$_{0.7}$[ZnO]$_{0.3}$}$_{1-x}${Tm$_2$O$_3$}$_x$ glass.
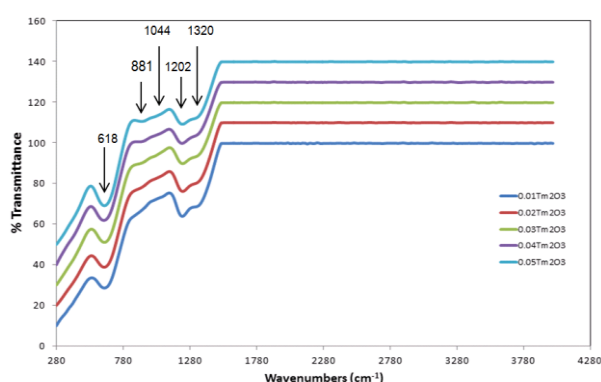
Fig. 2 FTIR spectra of {[(TeO$_2$)$_{0.7}$(B$_2$O$_3$)$_{0.3}$]$_{0.7}$[ZnO]$_{0.3}$}$_{1-x}${Tm$_2$O$_3$}$_x$ glass.

The FTIR spectra are shown in Fig 2. There are three major absorption bands observed that are in 600–640 cm^{-1}, 850–1100 cm^{-1} and 1200–1400 cm^{-1}. The band at 600–640 cm^{-1} is assigned for TeO$_4$ trigonal bipyramids [11]. It is noticed that the size of the peaks that correspond to the amount of TeO$_4$ increases as Tm^{3+} is increased. The peaks at 850–1100 cm^{-1} is attributed to stretching modes of [BO$_4$]$^-$ tetrahedral boron coordination. This peak is unrecognizable at lower concentration of Tm$_2$O$_3$. However, at 0.05 mol content Tm^{3+}, the peak can then be seen. The peak assigned for [BO$_3$]^0 formed at 1200–1400 cm^{-1}. This peak became shallower with the increment of Tm^{3+}. Hence, it can be concluded that as Tm$_2$O$_3$ is added into the glass system, bridging oxygen is formed and it can be confirmed with the formation of TeO$_4$ and BO$_4$ structural unit. ZnO bond is absent in this FTIR spectra. This may be due to the breaking of Zn–O bond within the sample. Tm–O bond does not exist which might be due to the low concentration of Tm$_2$O$_3$ that cannot be detected by the equipment [2].

XRD patterns for the prepared glass sample are shown in Fig 3. It is observed that there is no peak produced and confirmed the amorphous nature of the sample. The presence of a small hump indicates that the glass system has gone under structural relaxation and phase transformation within the glassy region [12]. The position of the hump also shows the position of peak that will be formed if the glass started to devitrify [13].

The absorption spectra of Tm$_2$O$_3$-doped zinc borotellurite glass obtained at room temperature is shown in Fig 4. From the figure, the information about absorption transition that occurred in the glass sample can be obtained. The peak that produced at 345, 460, 682 and 786 nm were transitions of electrons from ground energy level ^{3}H$_6$ to ^{1}D$_2$, ^{1}G$_4$, ^{3}F$_{2,3}$ and ^{3}H$_4$ respectively. The same peaks were also reported by Xiao et al. (2008) [14] and Balda et al. (2008) [15].
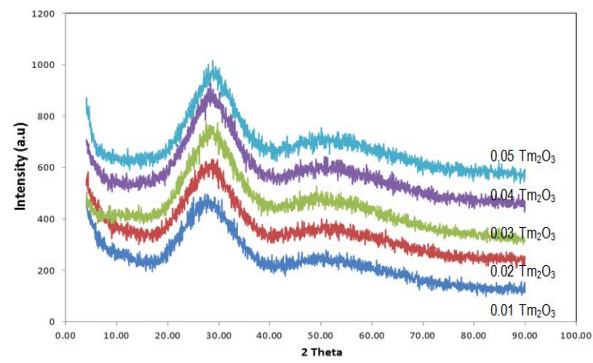
Fig. 3 XRD spectra of $\{[(TeO_2)_{0.7}(B_2O_3)_{0.3}]_{0.7}[ZnO_{0.3}]\}_{1-x}\{Tm_2O_3\}_x$ glass.

Table 1. Indirect E_{opt}, direct E_{opt}, cross-link density ($<n_c>$) and Urbach energy (ΔE) of the glass samples.

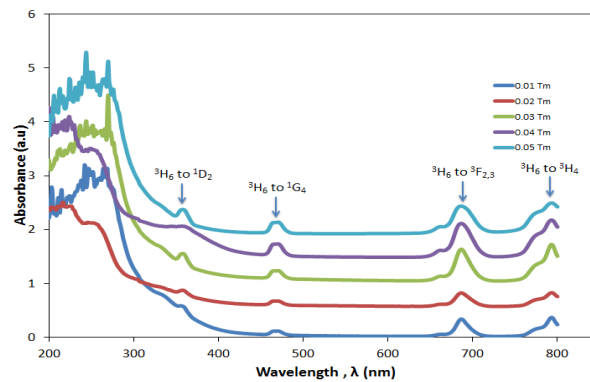| Tm$_2$O$_3$ composition (mol)	Indirect E_{opt} (eV)	Direct E_{opt} (eV)	$<n_c>$	ΔE (eV)
0.01	3.62	4.21	2.179	0.4450
0.02	3.79	4.38	2.209	0.4487
0.03	3.69	4.20	2.239	0.3978
0.04	3.78	4.37	2.268	0.4491
0.05	3.65	4.19	2.297	0.3828

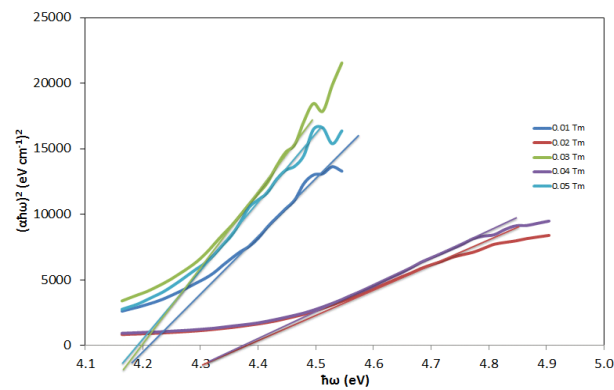Fig.4 Absorption spectra of $\{[(TeO_2)_{0.7}(B_2O_3)_{0.3}]_{0.7}[ZnO]_{0.3}\}_{1-x}\{Tm_2O_3\}_x$ glass.

Fig.5 Plot of $(\alpha\hbar\omega)^2$ vs $\hbar\omega$ for $\{[(TeO_2)_{0.7}(B_2O_3)_{0.3}]_{0.7}[ZnO]_{0.3}\}_{1-x}\{Tm_2O_3\}_x$ glass samples.
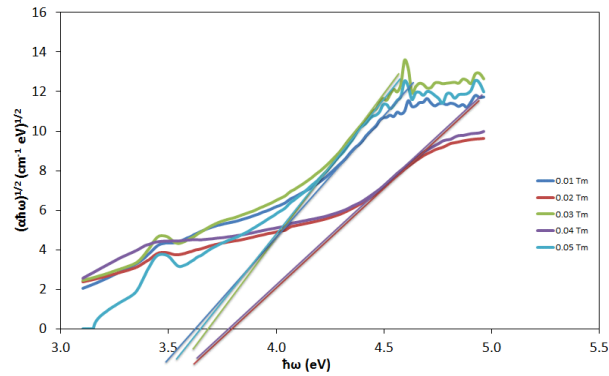
Fig.6 Plot of $(\alpha\hbar\omega)^{1/2}$ vs $\hbar\omega$ for $\{[(TeO_2)_{0.7}(B_2O_3)_{0.3}]_{0.7}[ZnO]_{0.3}\}_{1-x}\{Tm_2O_3\}_x$ glass samples.

      The variation of direct and indirect optical band gap are shown in Table 1. Direct and indirect optical band gap of the glass samples were found to be varied with the inclusion of thulium oxide. These changes might be due to the variation in the amount of bridging oxygens (BOs) and non-bridging oxygens (NBOs) in the glass system. According to Fares et al., (2014) [16], the decrement of NBOs causes a reduction in glass polarizability and increment of the optical band gap. This is because NBOs bound an excited electron less tightly as compared to BOs which causes NBOs to be more polarizable than the BOs. Besides that, the increase of E_{opt} also attributed to the increment of connectivity in the glass network after Tm is added. This was confirmed by the increase in the value of average cross-link density as shown in Table 1 [17]. Decrement of E_{opt} at 0.03 and 0.05 mol of Tm_2O_3 might be caused by weaker bond strength of thulium oxide compared to the other chemical oxides in the glass. As a result, it is easier for the electrons to jump into the conduction band [2]. Moreover, the existence of trivalent electrons, Tm^{3+} ions caused the increment in the number of free electrons in the glass network. This caused electrons to localize in deep energy levels and contributed to the declining of E_{opt} [18].

      Urbach energy gives information regarding defects and disorders that exist in the glass network [2]. In this present study, the trend of this data was found to be the same with the optical band gap. The values were increased at 2 and 4 mol% while decreased at 3 and 5 mol%. The augmentation was attributed to the increment of defects concentration in the glass system. According to Silins (1995) [19], defects in glass can be divided into three types that are intrinsic defects, impurity defects, and intrinsic impurity defects. Intrinsic defects are defects that arise from the atomic size local deviation from short range order. Impurity defects refers to the isolated impurity atoms or ions in the glass network while intrinsic impurity defects are complexes that consist of the impurity atoms that chemically bonded to one of the intrinsic defect atoms. The latter is the characteristics for doped glasses and this might be the type of defects that mostly exists within the glass under study. The reduction of ΔE at 3 and 5 mol% indicates the decrement of defects at that composition. This also showed that the glass was very stable at that point. Besides that, the structural units of TeO_4 and BO_4 can link together to form $BTeO_3$ and $BTeO_5$ which have higher connectivity and thus minimize defects.
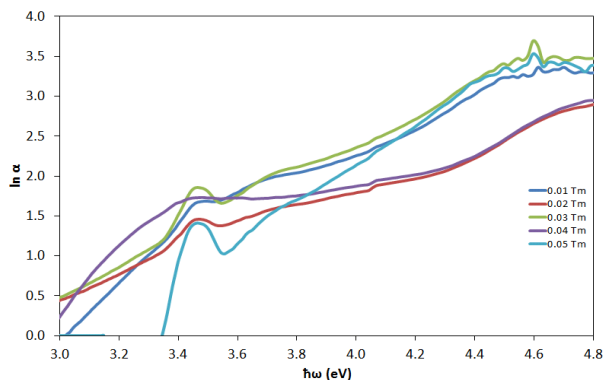
Fig.7 Plot of ln α vs ℏω for Tm_2O_3-ZnO-B_2O_3-TeO_2 glass samples.

The other parameters such as refractive index, molar refraction, and molar polarizability were determined. Refractive index is defined as the ratio of velocity of light in vacuum to the velocity of light in a specified medium. The velocity of light is slower in material with high density, it is expected that the refractive index is higher for a denser material compared to a material with lower density. It is important to study this parameter due to its connection with the electronic structure of amorphous material [20]. In addition, molar refraction (R_m) is a measure of the contribution of ionic packing in controlling the overall refractive index of glass while polarizability is the ability of electron clouds in atom to be distorted in the presence of an electric field. R_m is directly proportional to ionic polarizability of each constituent ion used in the glass. This is due to the fact that the increment of polarizability attributes to the rise of electrons in an atom. As light penetrates into the matter, it will interact with the electrons which causes the velocity of light to decrease and lead to the increment of molar refraction. Furthermore, molar polarizability is a measure of the total polarizability of a mole of a substance and is dependent on the temperature, index of refraction, and pressure.

The data of n, R_m and α_m are as listed in Table 2. The trend is similar for all three parameters and opposite to the trend of E_{opt} and ΔE. It increased at 3 and 5 mol% while decreased at 2 and 4 mol%. This variation might be due to the growth of packing density in the glass sample and confirmed by the inclination of cross-link density as shown in Table 1. This is also in agreement with the research done by Mallawany et al., (2008) [21]. When rare earth oxide was added into the host material, it would lead to the increase in packing density. As there was a direct relationship between density and refractive index, the value of refractive index also increased [22]. Besides that, the variation of molar polarizability is also the main contributing factor to the value of refractive index which is highly affected by cation polarizability and amount of BOs in the glass network. As Tm^{3+} (0.87 $Å^3$) with a higher polarizability replaced B^{3+} (0.003 $Å^3$) and Zn^{2+} (0.29 $Å^3$), it will cause molar polarizability to increase, together with molar refraction and refractive index. On the other hand, the formation of BOs that are known to be less polarizable compared to NBOs resulted in the reduction of the molar polarizability at 2 and 4 mol% as depicted in Fig 8 and thus leads to the decrement of n and molar refraction.

Based on the data that obtained from this work, it shows that this glass is suitable to be used as optical fiber since the high refractive index meet the conditions that required for the production of fiber core. The core must be in high refractive index than the cladding to insure that the light that transmits inside the fiber cable to undergo total internal reflection. Besides that, the glass also has a high potential to be apply as safety laser glass. This is based on its absorption spectra and optical band gap which show that the glass can absorb light with energy more than 3.62 eV and wavelength lower than 343 nm that can caused photokeratitis and photochemical cataract if exposed to human eye [23].

Table 2. Refractive index (n), molar refraction (R_m) and molar polarizability (α_m) of
$\{[(TeO_2)_{0.7}(B_2O_3)_{0.3}]_{0.7}[ZnO]_{0.3}\}_{1-x}\{Tm_2O_3\}_x$ glass samples.

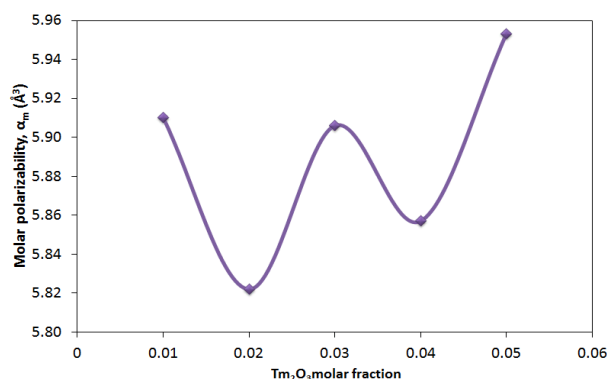| Tm_2O_3 composition (mol)	Refractive index, n	Molar refraction, R_m	Molar polarizability, α_m ($\mathring{A}^3$)
0.01	2.248	14.904	5.910
0.02	2.212	14.685	5.822
0.03	2.233	14.895	5.906
0.04	2.214	14.772	5.857
0.05	2.241	15.012	5.953

Fig.8 Molar polarizability of $\{[(TeO_2)_{0.7}(B_2O_3)_{0.3}]_{0.7}[ZnO]_{0.3}\}_{1-x}\{Tm_2O_3\}_x$ glass.

4. Conclusions

A series of quaternary tellurite glass system with composition $\{[(TeO_2)_{0.7}(B_2O_3)_{0.3}]_{0.7}[ZnO]_{0.3}\}_{1-x}\{Tm_2O_3\}_x\}$ was successfully prepared by melt-quenching technique. The addition of Tm_2O_3 to zinc borotellurite glass system was found to increase the density and molar volume of the glass.

Analysis on FTIR spectra shows that there is formation of bridging oxygens in the structure while XRD pattern confirmed the amorphous nature of the glass. It is also found that the optical properties of the glass varied independently with thulium oxide concentration and were influenced by BOs formation, cation polarizability, and also the packing density of the glass.

References

[1] M.K. Halimah, H. A. A. Sidek, W.M. Daud, H. Zainul, Z. A. Talib, A. W. Zaidan, A. S. Zainal, H. Mansor, Am. J. Appl. Sci **2**, 1541 (2005).
[2] M. N. Azlan, M. K. Halimah, S. Z. Shafinas, W. M. Daud, J. Nanomater **2013**, 1 (2013).
[3] H. Gebavi, D. Milanese, G. Liao, Q. Chen, M. Ferraris, M. Ivanda, O. Gamulin, S. Taccheo, J. Non. Cryst. Solids **355**, 548 (2009).
[4] Y. Tian, R. Xu, L. Zhang, L. Hu, J. Zhang, J. Appl. Phys **108**, 0 (2010).
[5] D. H. Cho, Y. G. Choi, K. H. Kim, Chem. Phys. Lett **332**, 263 (2000).
[6] V. C. V. Gowda, K. R. S. Pasha, M. S. Reddy, C. N. Reddy, Advanced **584**, 207 (2012).
[7] M. Seshadri, E. F. Chillcce, J. D. Marconi, F. A. Sigoli, Y. C. Ratnakaram, L. C. Barbosa,

J. Non. Cryst. Solids **402**, 141 (2014).

[8] N. Baizura, A. K. Yahya, J. Non. Cryst. Solids **357**, 2810 (2011).

[9] M. Khanisanij and H. A. A. Sidek, Adv. Mater. Sci. Eng **2014**, 1 (2014).

[10] S. Rada, A. Dehelean, and E. Culea, J. Non. Cryst. Solids **357**, 3070 (2011).

[11] R. S. Kundu, S. Dhankhar, R. Punia, K. Nanda, N. Kishore, J. Alloys Compd **587**, 66 (2014).

[12] A. K. Singh, K. Singh, N. S. Saxena, J. Ovonic Res **4**, 107 (2008).

[13] M. Thomas, Supplementary Cementing Materials in Concrete, Taylor and Francis Group, Boca Raton (2013).

[14] Z. Xiao, L. Yan, B. Zhou, F. Zhu, A. Huang, J. Wang, Journal of the Korean Physical Society **52**, 54 (2008).

[15] R. Balda, L. M. Lacha, J. Fernandez, M.A. Arriandiaga, J. M. Fernandez-Navarro, D. Munoz-Martin, Opt. Express **16**, 11836 (2008).

[16] H. Fares, I. Jlassi, H. Elhouichet, and M. Férid, J. Non. Cryst. Solids **396**, 1 (2014).

[17] A. H. Khafagy, A. A. El-Adawy, A. A. Higazy, S. El-Rabaie, A. S. Eid, J. Non. Cryst. Solids **354**, 3152 (2008).

[18] M. Altaf and M. Chaudhry, J. Korean Phys. Soc **36**, 265 (2000).

[19] A. R. Silins, Radiat. Eff. Defects Solids **134**, 7 (1995).

[20] J. N. Ayuni, M. K. Halimah, Z. A. Talib, H. A. A. Sidek, W. M. Daud, A. W. Zaidan, A. M. Khamirul, IOP Conf. Ser. Mater. Sci. Eng **17**, 012027 (2011).

[21] R. El-Mallawany, M. D. Abdalla, and I. A. Ahmed, Mater. Chem. Phys **109**, 291 (2008).

[22] S. Lakshimi, S. Rao, G. Ramadevudu, M. Shareefuddin, A. Hameed, M. N. Chary, M. L. Rao, Multicr. Int. J. Eng. Sci. Technol **4**, 25 (2012).

[23] Oregon State University, Laser Safety Training, http://oregonstate.edu/ehs/book/export/html/381, n.d (accessed 02.09.16).